Decomposition of Cyclohexanol on the Spinel System $CuCr_{2-x}Fe_xO_4$

Ashfaq Ahmed,* S. G. Oak,† and V. S. Darshane†

Department of Chemistry, Indian School, P.O.Box 558, Bahrain

†Department of Chemistry, Institute of Science, 15, Madam Cama Road, Bombay-400032, India

(Received November 18, 1994)

The System $CuCr_{2-x}Fe_xO_4$ has been studied with a view to correlate the catalytic behavior of spinels on the decomposition of cyclohexanol. All the compositions between $0.0 \leq x \leq 1.0$ had cubic symmetry and p-type semiconductivity except the compound $CuCr_2O_4$ ($x=0.0$) which showed tetragonal symmetry. The activation energy for the electronic conduction varied between 0.38 and 0.13 eV. The Seebeck coefficient (α) was found to increase with increases in 'x'. Catalytic evaluation was done in the temperature range 200—400 °C using cyclohexanol as a probe molecule. Our results show $CuCrFeO_4$ to be a better catalyst for cyclohexanol decomposition than $CuCr_2O_4$. The percent decomposition of alcohol increased with increases in mobility of charge carriers and decreases in values of activation energy. Further, dehydrogenation selectivity increased with increases in p-type behavior of the compositions from $CuCr_2O_4$ to $CuCrFeO_4$. X-ray and IR studies indicated that the spinel catalysts are quite stable over the temperature range investigated.

Ferrites have been used by various industries as catalysts for some industrially important catalytic reactions such as oxidative dehydrogenation of butene to butadiene and hydro-desulfurisation of crude petroleum and the treatment of automobile exhaust gasses.[1—3] For the conversion of butene to butadiene an inverse spinel, $MgFe_2O_4$, was found to be a better catalyst than a normal ferrite, $ZnFe_2O_4$.[4] Schwab et al.[5] have reported that normal ferrites are more active for carbon monoxide oxidation than the inverse ferrites. Gradation in the activity of the inverse ferrites have also been observed by Cares and Hightower,[6] who reported $CuFe_2O_4$ to be more active than $CoFe_2O_4$ for the conversion of butene to butadiene. Gallium-containing spinels have been investigated for nitrous oxide decomposition[7] and decomposition of 1-octanol,[8] while pure Ga_2O_3 has been reported as an effective catalyst for the decomposition of methyl cyclohexanol.[9] Catalytic properties of $CuCr_2O_4$ for cyclohexanol decomposition has been reported by Fridman et al.[10]

In a number of previous studies,[11—14] we have synthesized and characterized spinel ferrite systems. In this paper, we have attempted to study the decomposition of cyclohexanol using ferrite catalysts. Further, the ferrites containing Cu, Cr, and Fe have aroused considerable interest with regard to their valency and site distribution between tetrahedral and octahedral sites. We have studied $CuCr_{2-x}Fe_xO_4$ systems with a view to investigating the effects of substitution of Fe^{3+} on structural, electrical, and thermo-emf properties, and its subsequent effects on the catalytic activity in the decomposition of cyclohexanol. We have used X-ray diffraction, electrical conductivity, thermo-emf, and IR spectroscopic studies for the characterization of the catalysts.

Experimental

The various compositions of the catalysts $CuCr_{2-x}Fe_xO_4$ ($x=0.00$, 0.25, 0.50, 0.75, and 1.00) were prepared by the precursor method. Accurately weighed quantities of respective metal salts, ferric citrate, and citric acid were dissolved in a minimum amount of warm distilled water. The mixture containing individual metal salts and anhydrous citric acid was refluxed for 5 h. at 100 °C. Finally the refluxed solution was slowly evaporated to form a gel. This gel was dehydrated in an oven at 110 °C to obtain the citrate precursor, which later crumbled to a powder. The fine powder was calcined at 450 °C in a furnace for 6 h.

X-Ray diffraction patterns of the powdered catalysts were recorded on a Siemens D-500 Krystalloflex diffractometer with a microprocessor controller using nickel-filtered Cu $K\alpha$ radiation. X-Ray patterns of all compositions indicated the formation of single spinel phase. Pellets of the above catalysts were prepared using a 2.0% poly-vinyl acetate solution under 10000 psi (1 psi=8.894757×10^3 pa) pressure. Initially pellets were heated in air for 5 h to remove the binder and then heated at 900 °C, the sintering temperature, for 15 h. X-Ray intensity calculations were done for the *hkl* planes 220, 311, 222, and 422 using the formula

$$I = |F_{hkl}|^2 \cdot P \cdot l + \cos^2 2\theta / \sin^2 \theta \cos \theta$$

where notations have the usual meaning.

DC resistivity of the catalysts was measured using an LCR Marconi bridge with a two-probe technique. The end

faces of each pellet were coated with a thin layer of conducting silver paste and the resistivity was measured from RT to 500 °C. An electric field of 20 V cm^{-1} was applied across the pellet for these measurements.

Seebeck coefficient measurements were done after sandwiching a thick pellet between two Cu blocks. The temperature difference across the sample was measured using copper–constantan thermocouple and potential difference generated was measured using a microvoltmeter.

The IR spectra of fresh and used catalysts were recorded on a Perkin–Elmer FTIR-1600 spectrophotometer from 1000 to 300 cm^{-1} using KBr as a standard.

Each compound of the system was studied for its catalytic activity in the temperature range from 200 to 400 °C using a fixed-bed flow reactor as described earlier.[8] The reactor (25 cm long and 10 mm i.d.) made from Pyrex glass contained 3.0 gms of powder catalyst held between two glass-wool plugs surrounded by glass beads to facilitate heat exchange. The alcohol was fed into the reactor at a rate of 0.206 $cm^3\,min^{-1}$ with the help of a motor-driven syringe pump. After each run, the reactor was flushed with nitrogen to obtain an inert atmosphere. Cyclohexanol was used as the probe molecule. The products were collected and analyzed on a gas chromatograph and were further confirmed by GC-MS.

Results and Discussion

Catalyst Characterization: X-Ray Analysis: The results of the X-ray analysis are summarized in Table 1. It was observed that all the compounds of the system crystallized with cubic symmetry except x=0.0, which had a tetragonal nature. The values of lattice constants increased with increases in values of 'x' from $CuCr_2O_4$ to $CuCrFeO_4$ (Table 1). To discover the most probable cation distribution and its variation with composition the intensity ratios I_{222}/I_{422}, I_{220}/I_{311}, and I_{222}/I_{311} for different possible models were calculated, as reflections 222, 422, 311, and 220 are known to be sensitive to cation distribution at both the sites.[15] The observed and calculated intensity ratios for the compound $CuCrFeO_4$ using different models are summarized in Table 2. The model in which $Fe^{3+}_{0.75}Cu^{2+}_{0.25}$ at the tetrahedral site and $Cu^{2+}_{0.75}Fe^{3+}_{0.25}Cr^{3+}$ at the octahedral site shows better agreement between observed and calculated intensity ratios. The models of cation distribution selected gave the least value of the reliability factor, $R=|F_{hkl}|_{obsd}-|F_{hkl}|_{calcd}/|F_{hkl}|_{obsd}$, which varied between 0.07 and 0.52. No temperature correction had to be introduced in the intensity calculations since the oxidic spinels have high melting points and, therefore, thermal vibrations of the atoms at RT should have negligible effects.[16] From X-ray intensity calculations we propose the probable ionic configuration for the system $CuCr_{2-x}Fe_xO_4$ as:

$$Cu^{2+}_{y}Fe^{3+}_{1-y}[Cu^{2+}_{1-y}Fe^{3+}_{1+y-x}Cr^{3+}_{2-x}]O^{2-}_{4}$$

where 'x' and 'y' are fractions of Cr^{3+} and Cu^{2+} ions respectively. Ok and Kim[17] have studied the compound $CuCr_{0.1}Fe_{1.9}O_4$ using the Mössbauer technique and have reported the presence of Fe^{3+} and Cu^{2+} at both the sites.

Transport Properties Room temperature resistivity values of all the compounds of the system as a function of temperature varied between 10^6 and 10^3 ohm cm^{-1}. The electrical resistivity (ρ) vs. temperature behavior obeyed Wilson's law, $\rho=\rho_0 \exp(\Delta E/kT)$,

Table 1. Lattice Constants a, c, Activation Energy (ΔE), Seebeck Coefficient (α), Mobility of Charge Carriers (μ), and Number of Charge Carriers (n) Values for the Different Compositions of the System $CuCr_{2-x}Fe_xO_4$

Composition	a	c	ΔE	α	μ	n
x	Å	Å	eV	$\mu V\,K^{-1}$	$m^2\,V^{-1}\,s^{-1}$	cm^{-3}
0.00	6.039	7.868	0.38	+100.00	1.35×10^{-11}	4.51×10^{21}
0.25	8.28	8.28	0.25	+142.85	3.87×10^{-9}	1.61×10^{19}
0.50	8.32	8.32	0.21	+233.33	1.83×10^{-8}	3.48×10^{18}
0.75	8.36	8.36	0.17	+263.15	8.65×10^{-8}	7.50×10^{17}
1.00	8.37	8.37	0.13	+291.66	4.06×10^{-7}	1.61×10^{17}

Table 2. Cation Distribution for the Composition $CuCrFeO_4$

Cations at		I_{222}/I_{422}		I_{220}/I_{311}		I_{222}/I_{311}	
A-site	B-site	Obsd	Calcd	Obsd	Calcd	Obsd	Calcd
Fe^{3+}	$Cu^{2+}Cr^{3+}$	—	0.6142	—	0.5638	—	0.1126
$Fe^{3+}_{0.75}$	$Cu^{2+}_{0.75}Fe^{3+}_{0.25}$ Cr^{3+}	0.9444	0.9421	0.3900	0.3904	0.1700	0.1698
$Fe^{3+}_{0.5}$ $Cu^{2+}_{0.5}$	$Cu^{2+}_{0.5}Fe^{3+}_{0.5}$ Cr^{3+}	—	1.0447	—	0.6238	—	0.3643
$Fe^{3+}_{0.25}$ $Cu^{2+}_{0.75}$	$Fe^{3+}_{0.75}Cu^{2+}_{0.25}$ Cr^{3+}	—	3.8251	—	0.9019	—	0.8537
Cu^{2+}	$Fe^{3+}Cr^{3+}$	—	6.1118	—	1.0912	—	0.9986

indicating the semiconducting behavior of all the compounds. The activation energy values obtained from the linear plots of $\log\rho$ vs. $10^3/T$ for all the compositions of the system are listed in Table 1. Further, from the table it is observed that ΔE decreased from $CuCr_2O_4$ (0.38 eV) to $CuCrFeO_4$ (0.13 eV). The decrease in the activation energy values of the system can be attributed to the substitution of Fe^{3+} ions. Further, it can be seen that the conductivity behavior of the composition $CuCr_2O_4$ is due to the presence of Cu^{2+}/Cu^{1+} ion pairs. With increase in concentration of Fe^{3+} ions in the lattice of $CuCr_2O_4$, the number of Fe^{3+}/Fe^{2+} and Cu^{2+}/Cu^{1+} ion pairs increases, as is evident from ionic configuration, increasing electrical conductivity. The presence of Fe^{2+} ions in the ferrites causes a shoulder or splitting in infra-red absorption bands.[18] In the case of our compounds neither of the bands showed any shoulder or splitting, which may be due to the presence of very small concentrations of Fe^{2+} ions.

For calculation of mobility in the case of hopping carriers in oxidic semiconductors with localized states the following equation given by Heikes and Johnston[19] was used:

$$\mu = ed^2\nu\exp(-\Delta E/kT)/kT$$

where ΔE=activation energy, k=Boltzmann constant, d=jump length of charge carriers, taken as the average distance between neighboring octahedral sites, and ν= lattice frequency (obtained from the strongest IR band observed).

From Table 1 it is observed that the values of mobility showed an increasing trend with increases in value of Fe^{3+} ion concentration in the lattice. The electrical conductivity 'σ' is related to the number of charge carriers 'η', and their mobility 'μ' at RT by the relation, $\sigma=\eta e\mu$, where 'e' is the electronic charge. From this relation the number of charge carriers were calculated, which varied between 4.51×10^{21} for $CuCr_2O_4$ and 1.61×10^{17} cm^{-3} for $CuCrFeO_4$.

The plots of Δv vs. ΔT were used to find out the nature of charge carriers and Seebeck coefficient values. For the compositions with x=0.0 ($CuCr_2O_4$) the thermo-emf showed n-type behavior at low temperatures (below 100 °C) and p-type nature at high temperature. Seebeck coefficient values, which showed an increasing trend with increasing Fe^{3+} ion concentration, are reported in Table 1.

Infra-Red Studies: Two strong bands, ν_1 and ν_2, around 610 and 500 cm^{-1} respectively were shown by all the compositions of the system. The band positions and threshold frequencies for the different compositions of the system are listed in Table 3. The threshold frequency is for electronic transitions. The band positions agree with the values reported by earlier workers[20—23] for ferrite spinels. The higher frequency band (ν_1) is assigned to the tetrahedral group and lower frequency band (ν_2) can be assigned to the octahedral stretching vibrations.[8] The threshold frequency decreases from $CuCr_2O_4$ to $CuCrFeO_4$, which is in accordance with the trend observed for the activation energy (Table 1). With the substitution of Fe^{3+} ions in the lattice in the place of Cr^{3+} ions the frequency of stretching vibration shifts from 613 to 609 cm^{-1} (ν_1) and 511 to 485 cm^{-1} (ν_2). This shift in the band frequencies may be attributed to the migration of ions from B-sites to A-sites with increases in value of 'x'.

Catalytic Studies: The oxidative dehydrogenation of cyclohexanol over different catalyst compositions of the system is summarized in Table 4. It gave cyclohexanone as a dehydrogenation product and cyclohexane as a dehydration product as shown in Chart 1.

From Table 4, it is observed that conversion of cyclohexanol on $CuCrFeO_4$ is always greater at all temperatures compared to other catalyst compositions. It can also be seen from the table that decomposition of alcohol increases with increasing values of 'x' in the system. The conversion of cyclohexanol vs. temperature for various compositions of the system is given in Fig. 1. It is observed that conversion of cyclohexanol increases from $CuCr_2O_4$ to $CuCrFeO_4$. It is also noted that iron-rich catalysts are consistently more active than chromium-rich catalysts at all tempera-

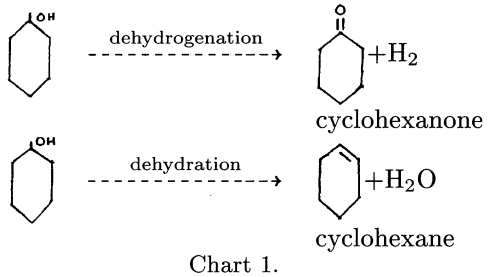

Chart 1.

Table 3. Band Positions and Threshold Frequencies for Different Compositions of the System $CuCr_{2-x}Fe_xO_4$

Composition	Absorption bands/cm^{-1}		Threshold frequency
x	ν_1	ν_2	
0.0	613	511	843
0.25	612	508	830
0.50	611	504	818
0.75	610	490	800
1.00	609	485	794

Table 4. Surface Area and Catalytic Performance Data for the Decomposition of Cyclohexanol over the Different Compositions of the System $CuCr_{2-x}Fe_xO_4$

Composition	Surface area	Catalytic bed	Conversion	Selectivity	
x	$m^2\,g^{-1}$	temperature/°C	%	Cyclohexanone	Cyclohexene
0.00	43.2	200	16.46	47.62	50.16
		300	32.89	43.99	55.71
		350	38.54	29.85	67.12
		400	42.51	23.81	73.14
0.25	52.6	200	21.45	66.78	31.16
		300	46.34	54.51	45.48
		350	57.56	41.72	56.56
		400	61.98	35.89	63.29
0.50	57.4	200	32.14	81.17	18.80
		300	53.26	77.65	22.29
		350	60.40	62.01	35.98
		400	67.98	38.91	59.01
0.75	64.7	200	38.99	86.32	10.62
		300	60.03	80.96	16.00
		350	72.56	67.67	30.15
		400	81.93	43.23	53.26
1.00	68.1	200	65.67	89.38	7.14
		300	77.41	84.19	11.80
		350	80.91	76.24	20.74
		400	88.64	62.43	35.26

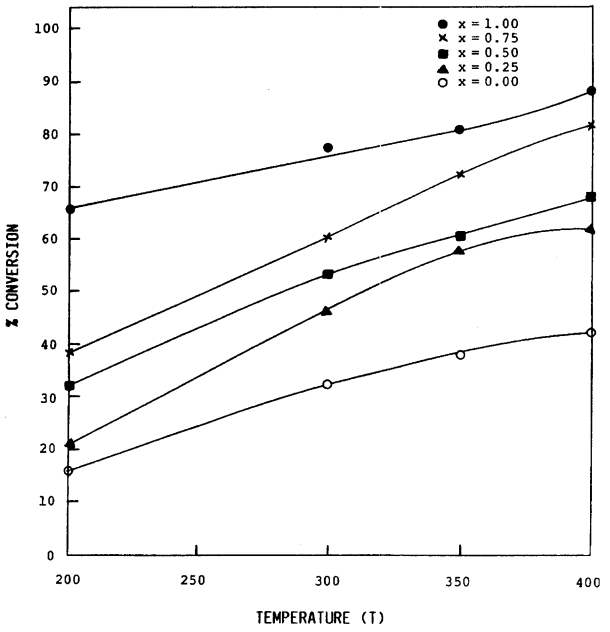

Fig. 1. Plot of % conversion vs. temperature for the system $CuCr_{2-x}Fe_xO_4$.

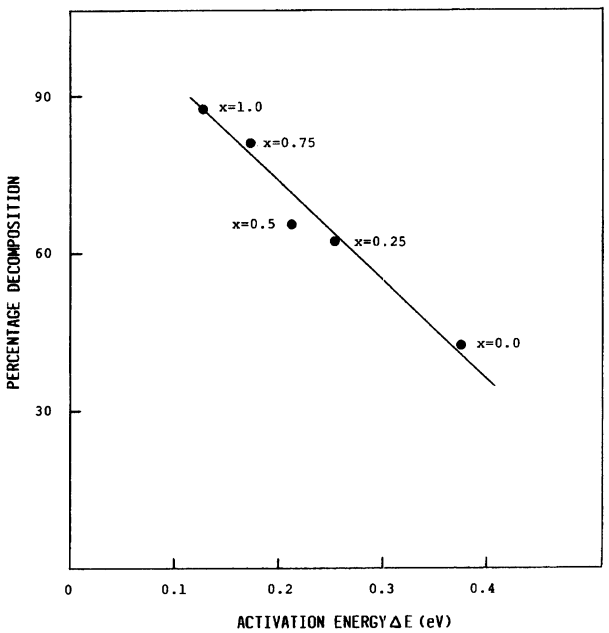

Fig. 2. Plot of % conversion vs. activation energy (ΔE) for the different compositions of the system $CuCr_{2-x}Fe_xO_4$.

tures studied. Further, from Table 4, it is observed that $CuCr_2O_4$ showed only 42.5% conversion, which increased to 67.9% for $CuCr_{1.5}Fe_{0.5}O_4$ and showed maximum conversion of 88.64% at 400 °C for $CuCrFeO_4$. The increase in activity from $CuCr_2O_4$ to $CuCrFeO_4$ can be explained on the basis of increase in number of active centres ($Fe^{3+}+Fe^{2+} \Longleftrightarrow Fe^{2+}+Fe^{3+}$).

The effects of electronic activation energy on the catalytic activity of spinels are shown in Fig. 2. From the figure it is observed that with decreasing values of activation energy from 0.38 eV (for $CuCr_2O_4$) to 0.13 eV (for $CuCrFeO_4$), the percent cyclohexanol decomposition increases. As catalysis involves transfer of electrons/holes from the surface of the catalyst to the substrate molecule and is reversible, the greater the activation energy, the more energy is required for the electronic transition and consequently the poorer will be the catalytic activity. Therefore, at 400 °C, $CuCr_2O_4$ (ΔE=0.38 eV) gave 42.51% conversion while

at the same temperature $CuCrFeO_4$ ($\Delta E = 0.13$ eV) gave 88.64% conversion.

Using the relation $\sigma = ne\mu$, it is observed that the number of charge carriers decreased with the increases in mobility (Table 1). Further since catalytic activity is dependent on the exchange of electrons/holes from the surface to the probe molecule, the greater the mobility, and the more easily the electrons/holes could be exchanged with cyclohexanol. This behavior is clearly reflected in the catalytic activity of the compositions from $x=0.0$ to 1.0. Thus, $CuCr_2O_4$ ($\mu = 1.3567 \times 10^{-11}$ $m^2 V^{-1} s^{-1}$) gave 38.54% conversion while $CuCrFeO_4$ ($\mu = 4.0653 \times 10^{-7}$ $m^2 V^{-1} s^{-1}$) gave 80.91% conversion at 350 °C.

The surface area of the different compositions of the system $CuCr_{2-x}Fe_xO_4$ was measured using the convential BET method at 77 K. From Table 4, it is observed that surface area of the compositions showed an increasing trend with increase in concentration of Fe^{3+} ions. This increase in surface areas with increasing values 'x' accounts for the increasing trend of catalytic activity.

Decomposition of alcohol on an oxide surface can be explained with the help of adsorption behavior suggested by various workers.[24,25] According to widely known conclusions based on electronic theory of catalysts the rate-limiting step for dehydrogenation is the migration of holes, while for dehydration it is migration of free electrons of the catalyst. Percent selectivity of cyclohexanone and cyclohexene vs. thermo-emf is plotted in Fig. 3. It is observed that cyclohexanone selectivity increases and cyclohekene selectivity decreases with increases in the value of the Seebeck coefficient. Thus, it can be seen that, at 200 °C, $CuCr_2O_4$ ($\alpha = +100.0$ $\mu V K^{-1}$) gave 47.62% dehydrogenation selectivity while at the same temperature $CuCrFeO_4$ ($\alpha = +291.66$ $\mu V K^{-1}$) gave 89.38% dehydrogenation selectivity. Such a correlation has also been reported in higher alcohols.[27]

The selectivity for dehydrogenation and dehydration can be explained with the help of the following mechanism:

The multiplet theory of catalysis implies two-point adsorption as a condition for alcohol adsorption on the catalyst.[28] In the case of oxide semiconductors, the oxygen of the hydroxyl group gets chemisorbed on the p-type surface by donating an electron and then the hydrogen of the hydroxyl group is lost to the surface as a proton. Later on, this proton combines with the hydrogen of the first carbon atom, leaving behind cyclohexanone as a dehydrogenated product. The various steps involved in the process are as follows (Chart 2):

In case of dehydration reactions by compositions with low concentrations of Fe^{3+}, the cyclohexanol gets adsorbed on the surface through the hydrogen atom of a neighboring (next to C–OH) carbon atom. This is followed by a loss of a proton to the surface and formation of carbanion (C^{-1}). However carbanion formed as an intermediate product is unstable and loses the –OH

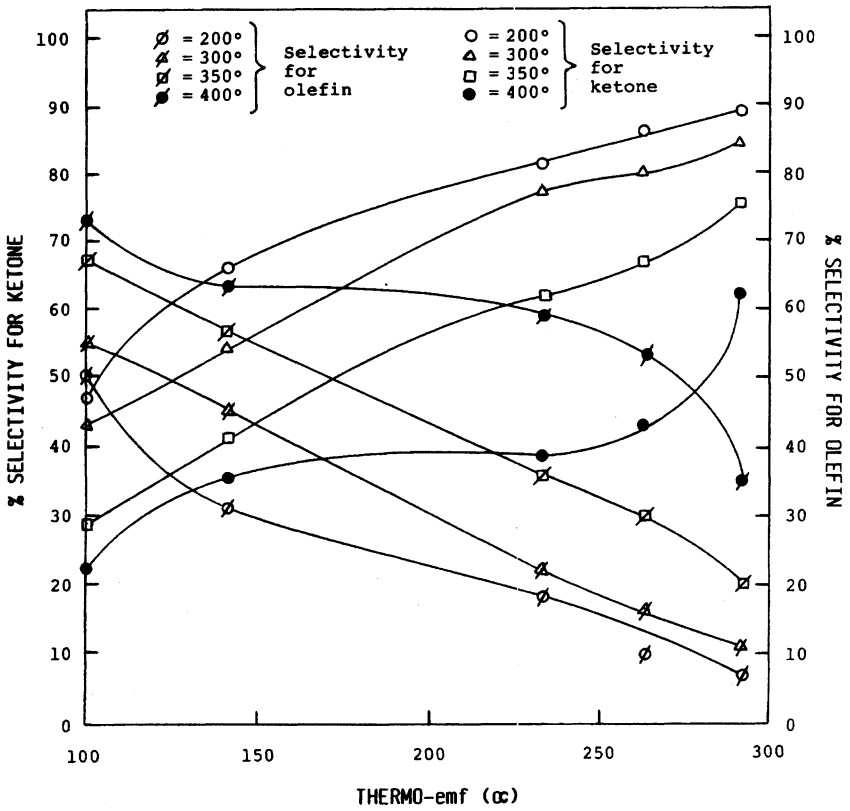

Fig. 3. Plot of % selectivity vs. thermo emf (α) for the different compositions of the system $CuCr_{2-x}Fe_xO_4$.

Table 5. Conversion Obtained after 15 h Process Time ($T=$ 400 °C. Flow rate = 0.206 $cm^3\,min^{-1}$) for the System $CuCr_{2-x}Fe_xO_4$

Composition	Conversion (%) after				
x	1 h	5 h	9 h	13 h	15 h
0.0	42.00	42.00	42.00	41.92	41.92
0.25	59.98	59.98	59.25	59.25	59.25
0.50	67.25	67.25	67.25	66.87	66.87
0.75	81.95	81.95	81.90	81.90	81.90
1.00	88.50	88.50	87.85	87.85	87.80

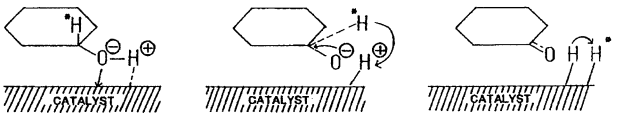

Chart 2.

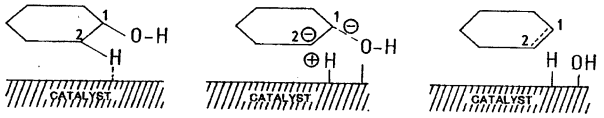

Chart 3.

group to the surface, thus forming an olefin and a water molecule. The various step are given in Chart 3:

Stability of the Catalysts Studied: The catalytic decomposition of cyclohexanol was done in nitrogen. To measure the stability of the catalysts, three checks were made (i) conversion level over a long period (process time 15 h after reaching steady state), (ii) comparison of IR spectra and (iii) comparison of the X-ray diffraction patterns of used catalysts with those of a fresh one.

The products were collected at intervals of 1 h after reaching steady state (constant conversion at this temperature). The results are summarized in Table 5. Further, from the table, it can be seen that conversion did not fall even after 15 h of process time. This allowed us to sustain the activity of spinels in terms of conversion over 15 h of process time to be measured.

IR spectra of the used catalysts did not show any appreciable change in the band frequencies. However, the Fe^{3+} ion-rich catalysts showed very little change in the band positions (2—5 cm^{-1}), indicating that the catalysts are fairly stable over the temperature range studied.

X-Ray diffraction patterns of used catalysts did not show any additional lines although there was a slight decrease in intensity as compared with fresh catalysts, indicating that there is no bulk reduction of the catalyst and the spinel structure is essentially retained under reduced conditions.

References

1) W. L. Kehl and R. J. Rennard, U. S. Patents 34507886 and 34507887 (1969).

2) P. N. Rylander, Jr., and W. J. Zimmerschied, U. S. Patent 2805187 (1957).

3) I. Keizo, T. Toshio, K. Maso, and A. Toshikazu, Jpn. Kokai Tokkyo Koho 74-102590; 75-123174; 47-120886 (1976).

4) R. J. Rennard and W. L. Kehl, *J. Catal.*, **21**, 292 (1971).

5) G. M. Schwab, E. Roth, C. H. Grinteoz, and N. Mavarakis, "Structure and Properties of Solid Surfaces," ed by R. Gomer and C. S. Smith, University of Chicago Press, Chicago, IL (1953).

6) W. R. Cares and J. W. Hightower, *J. Catal.*, **23**, 294 (1971).

7) F. Pepe, P. Porta, and M. Schiavello, "Reactivity of Solids," ed by J. Wood and N. G. Vannerberg, Plenum Press, New York (1976), and references cited therein.

8) G. R. Dube and V. S. Darshane, *J. Chem. Soc., Faraday Trans. 1*, **88**, 1299 (1992).

9) H. A. Dabbagh, C. G. Huges, and B. H. Davis, *J. Catal.*, **133**, 445 (1992).

10) V. Z. Fridman, L. N. Bedina, and I. Ya Petroiv, *Kinet. Katal.*, **29**, 621 (1988).

11) J. A. Kulkarni, K. Muraleedharan, J. K. Srivastava, V. R. Marathe, V. S. Darshane, C. R. K. Murthy, and R. Vijayraghavan, *J. Phys. C (Solid State Phys.)*, **18**, 2593 (1985).

12) P. S. Jain and V. S. Darshane, *Indian J. Chem., Sect. A*, **19A**, 1050 (1980).

13) M. N. Khan, A. Memon, C. A. Hogarth, A. Ahmed, B. A. Mulla, and V. S. Darshane, *Philos. Mag., Part B*, **62**, 103 (1990).

14) P. Nathwani and V. S. Darshane, *J. Phys. C (Solid State Phys.)*, **21**, 3191 (1988).

15) E. F. Bertaut, *Compt. Rend.*, **230**, 213 (1950).

16) R. K. Dutta and R. Roy, *J. Am. Ceram. Soc.*, **50**, 578 (1967); *Am. Mineral.*, **53**, 1456 (1968).

17) H. N. Ok and U. K. Kim, *Phys. Rev. B*, **36**, 5120 (1987).

18) V. R. K. Murthy, K. V. Reddy, and J. Shobhanadri, *Indian J. Pure Appl. Phys.*, **16**, 79 (1978).

19) R. R. Heikes and W. D. Johnston, *J. Chem. Phys.*, **26**, 582 (1957).

20) J. Preudhomme and P. Tarte, *Spectrochim. Acta, Part A*, **27A**, 961 (1971).

21) W. B. White and De Angelis, *Spectrochim. Acta, Part A*, **23A**, 985 (1967).

22) Y. Obi and H. Saito, *Phys. Status Solidi A*, **16**, 9 (1973).

23) M. Kataoka and J. Kanamori, *J. Phys. Soc. Jpn.*, **32**, 113 (1972).

24) K. Hauffe, *Adv. Catal.*, **7**, 251 (1955).
25) R. Venkatachalam and J. C. Kuriacose, *J. Sci. Ind. Res.*, **30**, 68 (1971).
26) O. V. Krylov, "Catalysis by Non-Metals," Academic Press, New York (1970).
27) G. R. Dube and V. S. Darshane, *J. Mol. Catal.*, **79**, 285 (1993).
28) A. A. Balandin, *Adv. Catal.*, **10**, 96 (1958).